ARTICLE

Aqueous Emulsion Polymerizations of Methacrylates and Styrene via Reversible Complexation Mediated Polymerization (RCMP)

Received 00th January 20xx,
Accepted 00th January 20xx

DOI: 10.1039/x0xx00000x

Weijia Mao,[a] Jit Sarkar,[a] Bo Peng,[b*] and Atsushi Goto[a*]

Reversible complexation mediated polymerization (RCMP) was successfully exploited in aqueous emulsion polymerization of methyl methacrylate (MMA). The polymerization behavior was comprehensively studied using a series of emulsifiers, alkyl iodide initiating dormant species, and catalysts. The optimized combination of these species generated stable polymer particles up to relatively high solid contents (up to nearly 50%) and achieved nearly quantitative initiation efficiency and low dispersity ($Đ$ = 1.1–1.3). The kinetic and mechanistic aspects of the polymerization were elucidated by the partitioning tests of the species in the aqueous and organic phases and the particle number analysis in the course of polymerization. The emulsion RCMP was amenable to not only MMA but also functional methacrylates and styrene. No use of transition metal or sulfur compounds, relatively high solid contents, good monomer versatility, and high chain-end fidelity achievable in the emulsion RCMP are attractive features for polymer material applications and industrial applications.

Introduction

Emulsion polymerization is an industrially important process owing to the efficient heat transfer, low viscosity, and high polymerization rate. Emulsion polymerization has extensively been studied in living radical polymerization (LRP) (also termed reversible deactivation radical polymerization), yielding polymers with predictable molecular weights and narrow molecular weight distributions.[1-3] There are some challenges in using LRP in emulsion polymerization compared with conventional radical polymerization. The transportation and partitioning of the initiating dormant species and catalysts in the dispersed and continuous phases are to be carefully considered to control the polymerization. Also importantly, oligomers are generated at an early stage of polymerization in LRP, making the dispersed phase (particles) hard to stabilize and often causing coagulation of the particles. This is in sharp contrast to conventional radical polymerization, where high molecular-weight polymers are generated throughout the polymerization and stabilize the particles even at an early stage of polymerization. Therefore, important issues in emulsion LRP are the choice of appropriate initiating dormant species and catalysts and the stabilization of the particles under optimized reaction conditions using proper emulsifiers (surfactants).

Since the pioneering work of the emulsion polymerization of *n*-butyl methacrylate,[4] atom transfer radical polymerization (ATRP) has been successfully used in emulsion,[5-7] mini-emulsion,[8-10] and micro-emulsion[11,12] polymerizations for various monomers. Emulsion ATRP has also been controlled by external stimuli such as photo irradiation and electrical current.[13-16]

Reversible addition–fragmentation chain-transfer (RAFT) polymerization has most widely been studied in water-borne system.[17] To overcome the initial instability of the particles, macroinitiators has been used as emulsifiers. Amphiphilic block copolymers generated from the macroinitiators efficiently stabilized the particles.[18-21] The obtained particles are often well-defined self-assemblies such as micelles, worms, and vesicles. This elegant process is called polymerization-induced self-assembly (PISA).[1-3,22-33] The obtained self-assemblies have been used as drug carriers and imaging particles for biomedical applications and as fillers for rheological improvement of resins, for instance.[30-33]

Nitroxide-mediated radical polymerization (NMP) was the first LRP that was applied in emulsion polymerization. Since then, emulsion NMP has extensively been explored.[34-37] Other LPR systems such as organotellurium mediated radical polymerization (TERP),[38-40] iodine transfer polymerization (ITP),[41,42] and reverse iodine transfer polymerization (RITP)[43,44] have also been successfully utilized in emulsion and mini-emulsion polymerizations. While these emulsion LRP systems are successful and useful, possible limitations are the use of transition metals as catalysts for ATRP, the odour of sulfur compounds used in RAFT, and the high temperature required in NMP.

[a]*Division of Chemistry and Biological Chemistry, School of Physical and Mathematical Sciences, Nanyang Technological University, 21 Nanyang Link, 637371 Singapore.*
[b]*BASF Advanced Chemicals Co., Ltd., R&D I, No 300, Jiangxinsha Road, 200137 Shanghai, China*
E-mail: agoto@ntu.edu.sg and bo.a.peng@basf.com
Electronic Supplementary Information (ESI) available: Materials, measurement, experimental procedures, polymerization results, and partitioning test. See DOI: 10.1039/x0xx00000x

Scheme 1. Reversible activation of RCMP.

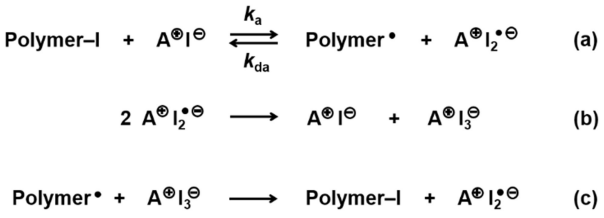

Our research group has developed reversible complexation mediated polymerization (RCMP), which is an LRP using a polymer-iodide (polymer–I) as a dormant species and an iodide anion (I^-), for example, as an activator catalyst.[45-47] Polymer–I coordinates I^- to form a halogen-bonding complex (polymer–I···I^-). The complex subsequently generates a propagating radical (polymer$^•$) and a deactivator ($I_2^{•-}$) (Scheme 1a). Because $I_2^{•-}$ is not a stable radical, two $I_2^{•-}$ species would react (disproportionate) to generate I^- and I_3^- (Scheme 1b). I_3^- works as a deactivator (Scheme 1c). The regenerated I^- works as an activator (Scheme 1a). I^- is used in the form of salts such as sodium iodide (NaI) and tetrabutylammonium iodide ($Bu_4N^+I^-$) (BNI). Advantages of RCMP include no use of heavy metals, sulfur compounds, or special capping agents, no requirement of high temperatures, and robust operation (no oxidation of catalysts in the air in the preparation of the polymerization mixture). RCMP is amenable to a wide range of hydrophobic and hydrophilic monomers in bulk and in solutions using organic solvents and water.[48-50] RCMP has also been combined with PISA (dispersion PISA system) to generate block copolymer self-assemblies.[51-53] However, RCMP has not been used in emulsion polymerization, which is important for industrial applications.

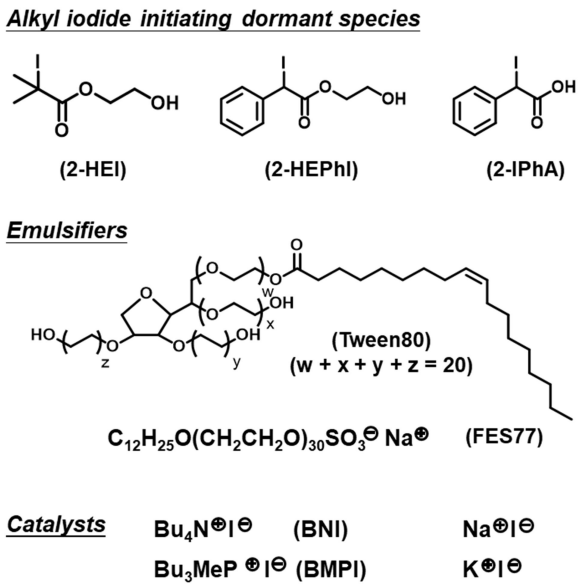

Fig. 1. Structures of alkyl iodides, emulsifiers, and catalysts used in this work.

Herein, we report the first emulsion RCMP. We studied the homopolymerizations of hydrophobic monomers in a water continuous phase. We achieved good stability of the particles using mixed (ionic and neutral) emulsifiers and good control in the polymerization. The studied monomers encompassed methyl methacrylate (MMA), styrene (St), and functional methacrylate monomers. We systematically studied the effects of the initiating dormant species and catalysts with different hydrophobicity in the polymerizations of MMA. The partitioning of the initiating dormant species in the continuous and dispersed phases and the change in the particle number were also studied for probing the mechanisms of the polymerization. Fig. 1 shows the studied alkyl iodide initiating dormant species, catalysts, and emulsifiers (surfactants) in this work.

Results and discussion

Polymerizations of MMA

Studies on emulsifier

As mentioned above, the stability of the particles is an important issue in emulsion LRP. We first studied emulsifiers in the polymerizations of MMA. We used a non-ionic emulsifier Tween80 (Fig. 1), which is non-toxic and biodegradable. We heated a mixture of MMA (monomer, 100 eq, 30.0 wt%), 2-hydroxyethyl 2-iodoisobutyrate (2-HEI (Fig. 1), an alkyl iodide initiating dormant species, 1 eq), NaI (catalyst, 1 eq), BNI (catalyst, 1 eq), 2,2'-azobis(2-methylpropionamidine) dihydrochloride (V50) (water-soluble azo initiator, 0.5 eq), Tween80 (emulsifier, 5.0 wt%), and water (solvent, 65.0 wt%) in a reaction vessel under a continuous argon flow using mechanical stirring at 60 °C. The small amount of V50 was added to increase the polymerization rate. Azo initiators are often used to decrease the deactivator concentration and hence effectively accelerate the polymerization in living radical polymerizations. The monomer conversion reached 52% for 1.5 h, and the number-average molecular weight (M_n) and dispersity $Đ$ (= M_w/M_n) values were 8100 and 1.21, respectively, where M_w is the weight-average molecular weight (Table 1 (entry 1) and Fig. 2 (squares)). However, the particles coagulated and precipitated during the polymerization. Thus, we studied an ionic emulsifier FES77 (1.7 wt%) (Fig. 1). FES77 bears a SO_3Na group similarly to sodium dodecyl sulfonate (SDS). Stable particles were generated, because of the electrostatic repulsion originated from FES77 that covered the particle surfaces. However, the $Đ$ value was relatively large (>1.50) (Table 1 (entry 2) and Fig. 2 (triangles)). Thus, we tried to combine Tween80 and FES77 (3/1 (w/w)) to seek both low dispersity and particle stability. Stable particles were generated and the $Đ$ value became relatively small (1.18–1.33). The monomer conversion reached ~100% for 100 min, giving a poly(methyl methacrylate) (PMMA) with M_n = 17000 and $Đ$ = 1.33 (Table 1 (entry 3) and Fig.2 (circles)). We reduced the amount of the emulsifier (Tween80/FES77 (3/1 (w/w))) from 3.3 wt% (Table 1 (entry 3)) to 0.7 wt% (Table 1 (entry 4)), resulting in a coagulation of particles and a large $Đ$ value (= 2.25). Hence, we utilized the mixture (3.3 wt%) of Tween80

and FES77 (3/1 (w/w)) in the following MMA polymerizations. V50 is a cationic azo initiator, which may associate with the anionic FES77 emulsifier. However, the optimized condition used the neutral emulsifier (Tween80) as well as the anionic emulsifier (FES77) in a mixed manner (3/1 (w/w)). Because of the relatively small fraction of the anionic FES77 emulsifier and the relatively small amount of V50, we observed no coagulation even using the cationic V50 azo initiator.

Studies on catalysts

In the mentioned Tween80/FES77 combined system (Table 1, entry 3), we co-used NaI and BNI. NaI is soluble in water and is expected to catalyze the polymerization in the water phase. BNI has four hydrophobic butyl groups and is more soluble in the organic phase and therefore is expected to catalyze the polymerization in the organic phase. BNI is also amphiphilic. BNI is slightly soluble in water and may also play some role in catalyzing the polymerization in the water phase.

Mechanistically, in the beginning of polymerization, the hydrophobic MMA monomer would form droplets, which are dispersed in water, and emulsifiers would form micelles in water. At an early stage of polymerization, MMA molecules would diffuse from the monomer droplets to the micelles, and also MMA molecules slightly dissolved in water would polymerize from the 2-HEI initiating dormant species dissolved in water to generate oligomers, which would also enter the micelles. 2-HEI and catalysts may also diffuse into the micelles and initiate the polymerization in the micelles. Through these processes, nucleation would occur. Subsequently, MMA molecules would continue to diffuse from the monomer droplets to the particles, and the polymerization would mainly occur in the particles (organic phase).

Table 1. Emulsion Polymerizations of MMA using different emulsifiers and catalysts.

Entry	Target DP[a]	Emulsifier	Catalysts A / B	$[MMA]_0/[2\text{-HEI}]_0/[A]_0/[B]_0/[V50]_0$ (mM)	T (°C)	t (min)	conv (%)	M_n ($M_{n,theo}$[b])	$Đ$
1	100	Tween80[c]	NaI / BNI	8000/80/80/80/40	60	90	52	8100 (5200)	1.21
2	100	FES 77[d]	NaI / BNI	8000/80/80/80/40	60	90	93	17000 (9300)	1.70
3	100	Tween80 / FES77[e,f]	NaI / BNI	8000/80/80/80/40	60	100	100	17000 (10000)	1.33
4	100	Tween80 / FES77[e,g]	NaI / BNI	8000/80/80/80/40	60	100	77	11000 (7700)	2.25
5	100	Tween80 / FES77[e,f]	none	8000/80/0/0/40	60	20	100	53000 (10000)	2.39
6	100	Tween80 / FES77[e,f]	NaI / none	8000/80/160/0/40	60	60	100	25000 (10000)	1.54
7	100	Tween80 / FES77[e,f]	none / BNI	8000/80/0/160/40	60	120	59	26000 (5900)	1.30
8	100	Tween80 / FES77[e,f]	KI / BNI	8000/80/80/80/40	60	100	100	16000 (10000)	1.38
9	100	Tween80 / FES77[e,f]	NaI / BMPI	8000/80/80/80/40	60	100	100	19000 (10000)	1.49

[a]Target degree of polymerization (DP) at 100% monomer conversion as calculated according to $[MMA]_0/[2\text{-HEI}]_0$. [b]Theoretical M_n value calculated according to ($[MMA]_0/[2\text{-HEI}]_0$) × (monomer conversion) × (molecular weight of MMA). [c]$[MMA]_0/[Tween80]_0/[water]_0$ = 30.0/5.0/65.0 (w/w/w). [d]$[MMA]_0/[FES77]_0/[water]_0$ = 30.0/1.7/68.3 (w/w/w). [e]Tween80/FES77 = 3/1 (w/w). [f]$[MMA]_0/[emulsifier]_0/[water]_0$ = 30.0/3.3/66.7 (w/w/w). [g]$[MMA]_0/[emulsifier]_0/[water]_0$ = 30.0/0.7/69.3 (w/w/w).

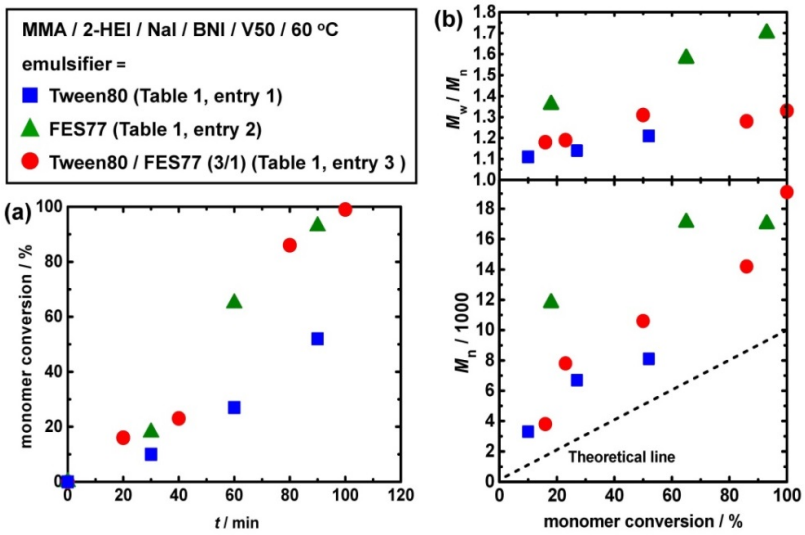

Fig. 2. Plots of (a) monomer conversion vs t and (b) M_n and M_w/M_n vs monomer conversion for the MMA/2-HEI/NaI/BNI/V50 systems using different emulsifiers (60 °C): $[MMA]_0$ = 8 M; $[2\text{-HEI}]_0$ = 80 mM; $[NaI]_0$ = 80 mM; [BNI] = 80 mM; $[V50]_0$ = 40 mM (Table 1, entries 1-3). The symbols are indicated in the figure.

To probe the roles of NaI and BNI, we studied no use of catalyst and single use of NaI or BNI. In the absence of any catalysts, the M_n value (53,000) largely deviated from the theoretical value (10,000) and the $Đ$ value was as large as 2.39 (Table 1, entry 5), showing no control of the polymerization. In this system, the polymerization was induced by the azo initiator (V50). Because of the use of the alkyl iodide dormant species, degenerative chain transfer could operate. However, the degenerative chain transfer constant in the MMA polymerization is not so large (2.6 at 80 °C and 1.6 at 90 °C)[54,55] that a small $Đ$ value could not be achieved in this system.

Fig. 3 and Table 1 (entries 3, 6, and 7) compare the results with dual use of NaI and BNI, single use of NaI, and single use of BNI. The single use of NaI afforded polymers with relatively large $Đ$ values (~1.5) throughout the polymerization (Fig. 3 (triangles) and Table 1 (entry 6)), probably because of the lack of a sufficient amount of catalyst in the organic (particle) phase. The single use of BNI led to relatively small $Đ$ values (1.18-1.33) but gave large deviation of the M_n values from the theoretical values by a factor of 4-10 (Fig. 3 (squares) and Table 1 (entry 7)), suggesting the low initiation efficiency from the alkyl iodide (2-HEI). The low initiation efficiency would be ascribed to the lack of a sufficient amount of catalyst in the water phase to initiate 2-HEI present in water. As already described, the dual use of NaI and BNI resulted in relatively small $Đ$ values (1.18-1.33) and at the same time gave relatively small deviation in the M_n values (Fig. 3 (circles) and Table 1 (entry 3)). The presence of the catalysts in both water (NaI) and organic (BNI) phases is important.

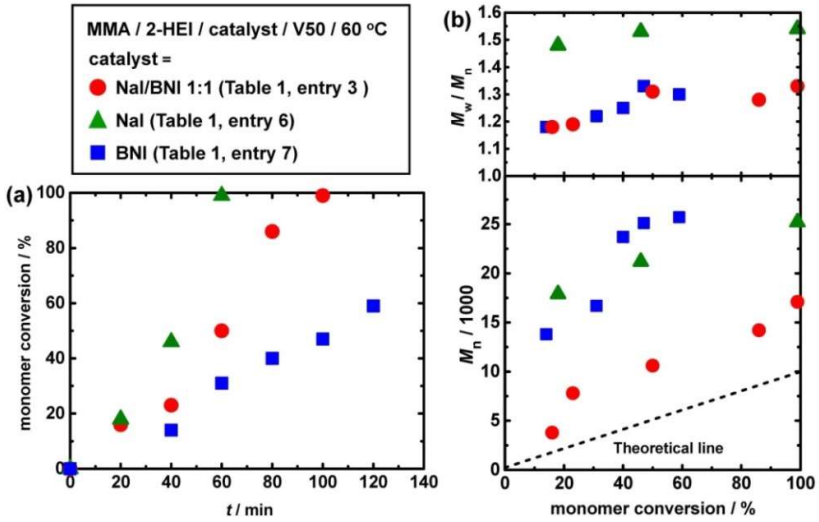

Fig. 3. Plots of (a) monomer conversion vs t and (b) M_n and M_w/M_n vs monomer conversion for the MMA/2-HEI/Catalyst/V50 systems using a mixture of Tween80 and FES77 emulsifiers (60 °C): $[MMA]_0$ = 8 M; $[2\text{-HEI}]_0$ = 80 mM; $[catalyst]_0$ = 160 mM; $[V50]_0$ = 40 mM (Table 1, entries 3, 6, and 7). The symbols are indicated in the figure.

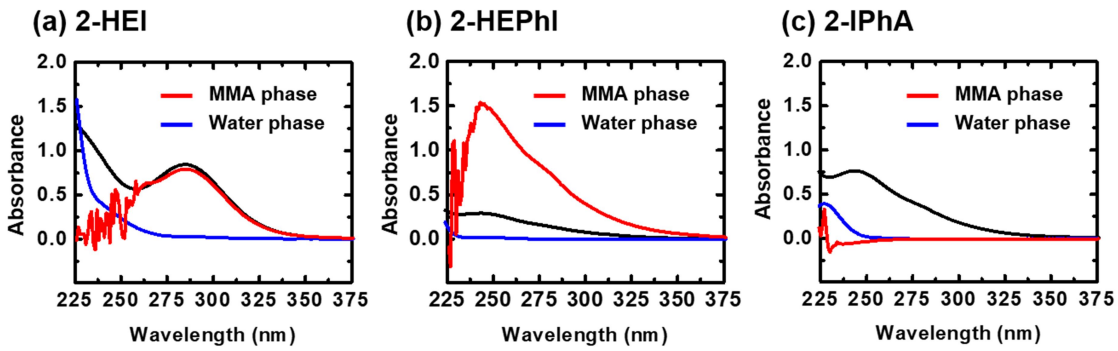

Fig. 4. UV-Vis spectra for partitioning tests of (a) 2-HEI, (b) 2-HEPhI, and (c) 2-IPhA present in the MMA phase (red line) and the water phase (blue line). Each phase was diluted with methanol (1000 times). The black line represents the alkyl iodide in methanol (0.004 wt% in methanol) for reference.

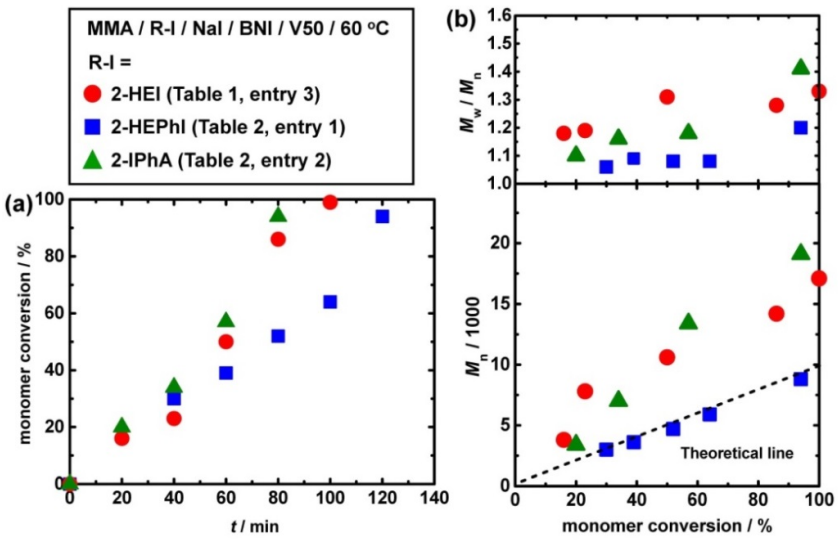

Fig. 5. Plots of (a) monomer conversion vs t and (b) M_n and M_w/M_n vs monomer conversion for the MMA/R-I/NaI/BNI/V50 systems using a mixture of Tween80 and FES77 emulsifiers (60 °C): $[MMA]_0$ = 8 M; $[R\text{-}I]_0$ = 80 mM; $[NaI]_0$ = 80 mM; $[BNI]_0$ = 80 mM; $[V50]_0$ = 40 mM (Table 1, entry 3, and Table 2, entries 1 and 2). The symbols are indicated in the figure.

Table 2. Emulsion polymerizations of MMA using Different Alkyl Iodide Initiating Dormant Species (R-I).[a]

Entry	Target DP[b]	R-I	$[MMA]_0/[R\text{-}I]_0/[NaI]_0/[BNI]_0/[V50]_0$(mM)	T (°C)	t (min)	conv (%)	M_n ($M_{n,theo}$)[c]	$Đ$
1[d]	100	2-HEPhI	8000/80/80/80/40	60	120	94	8800 (9400)	1.20
2[d]	100	2-IPhA	8000/80/80/80/40	60	80	94	19000 (9400)	1.41
3[d]	200	2-HEPhI	8000/40/160/160/20	60	240	100	18000 (20000)	1.29
4[d]	400	2-HEPhI	8000/20/160/160/10	60	240	70	25000 (28000)	1.34
5[d]	800	2-HEPhI	8000/10/160/160/10	60	480	82	32000 (65000)	1.27
6[e]	100	2-HEPhI	8000/80/80/80/40	60	120	95	7100 (9500)	1.14
7[f]	100	2-HEPhI	8000/80/80/80/40	60	180	100	11000 (10000)	1.28
C1	100	2-HEPhI	8000/80/80/80/40 (in bulk)	60	150	25	3700 (2500)	1.10

[a]The emulsifier was Tween80/FES77 = (3/1 (w/w)). [b]Target degree of polymerization (DP) at 100% monomer conversion as calculated according to $[MMA]_0/[R\text{–}I]_0$. [c]Theoretical M_n value calculated according to ($[MMA]_0/[R\text{–}I]_0$) × (monomer conversion) × (molecular weight of MMA). [d]$[MMA]_0/[emulsifier]_0/[water]_0$ = 30.0/3.3/66.7 (w/w/w). [e]$[MMA]_0/[emulsifier]_0/[water]_0$ = 40.0/4.4/55.6 (w/w/w). [f]$[MMA]_0/[emulsifier]_0/[water]_0$ = 50.0/5.6/44.4 (w/w/w).

We also studied combinations of other catalysts. We combined BNI with potassium iodide (KI) instead of NaI (Table 1 (entry 8) and Fig. S2 (squares) in ESI) and combined NaI with tributylmethylphosphonium iodide (BMPI) instead of BNI (Table 1 (entry 9) and Fig. S2 (triangles) in ESI). These systems afforded similar results to that using NaI and BNI (Table 1 (entry 3)), generated polymers with $Đ$ = 1.38-1.49. The results suggest a wide catalyst scope in the present system. In what follows, we kept using the combination of NaI and BNI.

Studies on Alkyl Iodide Dormant Species

2-HEI (alkyl iodide dormant species) bears a hydroxyl group and has an amphiphilic nature. We also studied more hydrophobic 2-hydroxyethyl 2-Iodo-2-phenylacetate (2-HEPhI) bearing an aromatic ring (Fig. 1) and hydrophilic 2-iodo-2-phenylacetic acid (2-IPhA) bearing a carboxylic acid (Fig. 1).

We carried out a partitioning test of 2-HEI, 2-HEPhI, and 2-IPhA in organic and aqueous phases. We vigorously stirred a mixture of MMA (6 g, 100 eq), alkyl iodide (1 eq), and water (12 g) at 60 °C for 30 min (with no surfactant). After 30 min, the stirring was stopped to separate out the organic (MMA) and aqueous phases at 60 °C for 10 min. Each phase was then 1000 times diluted with methanol, and the UV-Vis absorption was measured. Fig. 4 shows the absorption spectra of the MMA phase (red lines) and aqueous phase (blue lines) for 2-HEI (Fig. 4a), 2-HEPhI (Fig. 4b), and 2-IPhA (Fig. 4c). Black lines (Fig. 4) show the alkyl iodides in pure methanol for reference. The alkyl iodides had an absorption peak at 284 nm (2-HEI) or 243 nm (2-HEPhI and 2-IPhA), and their absorption tailed to

approximately 350 nm. From the absorbance in the MMA (red lines) and aqueous phases (blue lines), we calculated the partition of the alkyl iodides in each phase. For 2-HEI, 96% of 2-HEI was present in the MMA (6 g) phase and 4% of 2-HEI was present in the aqueous (12 g) phase. While 2-HEI is amphiphilic, the result shows that 2-HEI tends to be soluble in an organic phase more than in an aqueous phase. (The absolute solubility of 2-HEI in water was 24.6 g/L.) The partition of 2-HEPhI was virtually 100% in the MMA phase, as expected from the hydrophobic nature of 2-HEPhI. The partition of 2-IPhA was virtually 100% in the aqueous phase, also as expected from the hydrophilic nature of 2-IPhA.

We compared the polymerizations using 2-HEI (Fig. 5 (circles) and Table 1 (entry 3)), 2-HEPhI (Fig. 5 (squares) and Table 2 (entry 1)), and 2-IPhA (Fig. 5 (triangles) and Table 2 (entry 2)). While the M_n values somewhat deviated from the theoretical values in the 2-HEI system (Fig. 5 (circles)), the M_n values almost perfectly matched the theoretical values in the 2-HEPhI system (Fig. 5 (squares)), indicating a high and almost quantitative initiation from 2-HEPhI. 2-HEPhI is hydrophobic but bears a hydroxyl group and may still diffuse through the aqueous phase. A part of 2-HEPhI would initiate in the aqueous phase to generate oligomers, which can enter the micelles, and the rest of 2-HEPhI would be captured in the micelles and initiate inside the micelles. 2-HEPhI is more hydrophobic than 2-HEI and would efficiently be captured in the micelle. The capture of 2-HEPhI and oligomers in the micelles seemed quantitative, which would result in the nearly quantitative initiation. Another important factor would be the initiation (activation) rate. We previously experimentally determined the activation rate constant k_a (Scheme 1a) of several alkyl iodides (R-I) catalyzed by BMPI at 70 °C. The k_a value for R = phenylacetate (13×10^{-3} M^{-1} s^{-1}) was approximately 6 times larger than that for R = isobutyrate (2.3×10^{-3} M^{-1} s^{-1}).[56] While the absolute k_a values depend on the catalyst (NaI and BNI in the present work) and temperature (60 °C in the present work), the kinetic result suggests that the initiation of 2-HEPhI with R = phenylacetate is faster than that of 2-HEI with R = isobutyrate in the present system. The faster initiation of 2-HEPhI would also contribute to the higher initiation efficiency of 2-HEPhI than that of 2-HEI.

In contrast, the use of the hydrophilic 2-IPhA resulted in a deviation of the M_n values from the theoretical values (Fig.5 (triangles)), although 2-IPhA has a phenylacetate structure as 2-HEPhI does. 2-IPhA tends to be partitioned in the aqueous phase, as mentioned above. Thus, 2-IPhA would not efficiently be captured in the micelle, which would explain the deviation of the M_n value (lower initiation efficiency).

Among all of the studied conditions (described above), the 2-HEPhI system using NaI and BNI as catalysts with Tween80 and FES77 as emulsifiers was the most optimized system (Fig. 5 (squares) and Table 2 (entry 1)). The M_n value well matched the theoretical value, and the $Đ$ value was as low as 1.06-1.20 throughout the polymerization (up to 94% monomer conversion). The polymerization was also fast, as the monomer conversion reached 94% in 120 min.

The polymerization rate in the emulsion polymerization (Table 2 (entry 1)) was faster than that in the corresponding bulk polymerization (Table 2 (entry C1)). The polymerization rate in emulsion LRP is generally characterized by the segregation effect and the confined space effect.[1,57-61] The segregation effect increases the polymerization rate. It is a phenomenon that propagating radicals in separated particles are segregated and can not undergo termination (hence promote the polymerization). The observed increased polymerization rate would be explained by the segregation effect. The confined space effect decreases the polymerization rate and can operate when the particle size is small. RCMP contains deactivators ($I_2^{\bullet-}$ and I_3^-) (Scheme 1), and their concentrations should be higher than that of the propagating radicals because of the so-called persistent radical effect.[62,63] The confined space effect operates when the particle size is so small (<15 nm, for example)[57,61] that even one deactivator molecule in one particle exceeds the corresponding bulk concentration of deactivator. In such a case, the deactivation rate in the emulsion system is larger than that in the bulk system, which brings about a decreased polymerization rate. The observed particle sizes in the present work were typically 122-190 nm, as shown below. Therefore, the confined space effect would hardly operate in the present emulsion RCMP.

Table 3. Solid Content and Particle Number in Emulsion Polymerization of MMA.[a]

Entry	$[MMA]_0/[2\text{-HEPhI}]_0/[NaI]_0/[BNI]_0/[V50]_0$ (mM)[b]	T (°C)	t (min)	conv (%)	Solid content (PMMA and emulsifier) (%)	Particle diameter (DLS) (nm)	Particle number calculated from solid content (PMMA and emulsifier) (particles/g)	Particle number calculated from PMMA only (particles/g)
1	8000/80/80/80/40	60	40	30	10.7	122	9.8×10^{13}	6.5×10^{13}
			60	39	14.2	164	5.3×10^{13}	4.0×10^{13}
			80	52	18.8	142	10.1×10^{13}	8.7×10^{13}
			100	64	24.0	164	8.9×10^{13}	7.5×10^{13}
			120	94	28.6	190	6.8×10^{13}	5.9×10^{13}

[a]The same system as Table 2 (entry 1). [b]$[MMA]_0/[emulsifier]_0/[water]_0$ = 30.0/3.3/66.7 (w/w/w). The emulsifier was a mixture of Tween80 and FES77 (3/1 (w/w)).

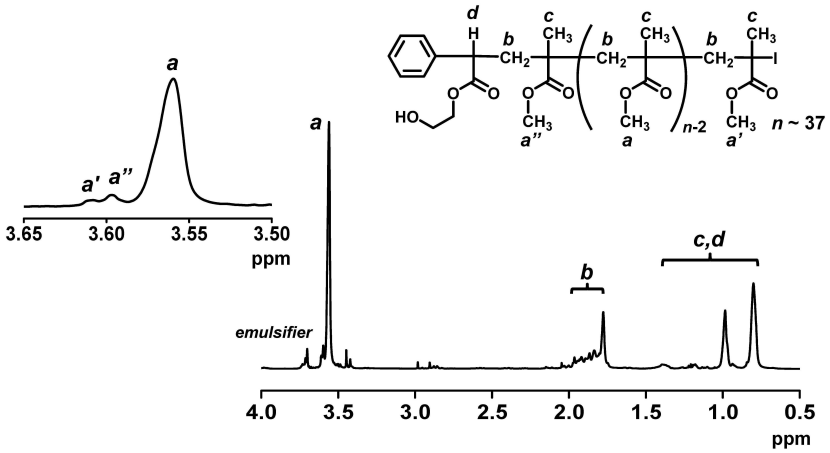

Fig. 6. ^{1}H NMR spectrum ($CDCl_3$) of PMMA-I obtained in Table 2 (entry 1) after 60 min (M_n= 3900 and $Đ$ = 1.09 after purification).

Study on Nucleation

A possible mechanism of the nucleation in the present system is as follows. This is a possible mechanism and other nucleation mechanisms may also operate. As mentioned above, in the beginning of the polymerization, hydrophobic MMA monomer droplets are dispersed in water. Emulsifiers form micelles in water. At an early stage of polymerization, MMA molecules diffuse from the monomer droplets to the micelles, and also MMA molecules slightly dissolved in water would polymerize from alkyl iodide initiating dormant species dissolved in water to generate oligomers, which would enter the micelles. Alkyl iodide initiating dormant species and catalysts may also diffuse into the micelles and initiate the polymerization in the micelles. Through these processes, nucleation would occur. The nucleation would usually be complete at an early stage of polymerization. Subsequently, MMA molecules continue to diffuse from the monomer droplets to the particles, and the polymerization would mainly occur in the particles. If this mechanism operates, the number of the particles would remain constant throughout the polymerization after the nucleation stage.

To probe the mechanism, we calculated the number of the particles in a representative system shown in Table 2 (entry 1), where the M_n values well matched the theoretical values and the $Đ$ values were ≤ 1.20 throughout the polymerization (up to a 94% monomer conversion). An aliquot of the polymerization mixture was taken out at 40, 60, 80, 100, and 120 min of the polymerization, dried completely, and weighed, from which the solid content (sum of PMMA and emulsifier) was calculated (Table 3). Another aliquot was taken out at each time, diluted with water (25 times), and analyzed with dynamic light scattering (DLS). The DLS intensity-distribution curve (Fig.S1 in ESI) showed a mono-modal peak for all studied samples, and the peak-top particle size was 122-190 nm (Table 3). Assuming that the peak-top particle size is the diameter of the particle and all of the emulsifier was used to cover the particle, and using 1.19 g/cm^3 for the density of PMMA[64] and 1.06 g/cm^3 for the average density of Tween80 and FES77,[65,66] we calculated the number of particle in 1 g of the polymerization mixture. The number of the particles (5.3×10^{13}–10.1×10^{13} particles/g) was in nearly the same order of magnitude at all studied polymerization times (above the 30% monomer conversion) (Table 3). The result suggests that the nucleation completed at an early stage of polymerization (below the 30% monomer conversion) and the number of the particles was virtually constant thereafter, as expected from the mentioned mechanism. (If we assume no emulsifier attached on the particle, the number of the particles was 4.0×10^{13}–8.7×10^{13} particles/g (Table 3). The order of magnitude is the same and the number of the particles is virtually constant at all polymerization times on this assumption, too. The actual number of particles (actual amount of emulsifier attached on the particle) would be between those on the two assumptions.)

Chain-end fidelity

We studied the iodide chain-end fidelity (livingness) of a PMMA-iodide (PMMA-I) synthesized in the representative system shown in Table 2 (entry 1). The polymer obtained at 60 min was purified by the reprecipitation (in a mixture of methanol and water (2/1 (v/v))) and further purified using preparative gel permeation chromatography (GPC) (M_n = 3900 and $Đ$ = 1.09 after purification). Fig. 6 shows ^{1}H NMR spectrum of the purified polymer. The methoxy protons (OCH_3) at the side chain (*a*, *a'*, and *a''*) appeared at 3.53-3.62 ppm. The main peak at 3.53-3.59 ppm is assigned to the repeating monomer units (*a*) in the middle of the chain. The terminal chain end unit (*a'*) adjacent to the iodide chain end appeared at 3.60-3.62 ppm, and the terminal chain end unit (*a''*) adjacent to the initiating 2-HEPh chain end appeared at 3.59-3.60 ppm. According to the ^{1}H NMR peak area and the M_n value (= 3900), the fraction of the iodide chain end was calculated to be nearly 100% (98% as calculated) with an experiment error, suggesting a high iodide chain-end fidelity. A small amount of dead polymers should be generated via radical-radical termination because the polymerization is a radical polymerization. V50 (0.5 equiv to 2-HEPhI) should also generate new chains,

although the amount of the new chains would be relatively small because only 20% of V50 (hence 0.1 equiv to 2-HEPhI) decomposed for 60 min at the studied temperature of 60 °C and not all but a part of the generated radicals generate polymers or enter the particles. Nevertheless, the result suggests that the amount of the dead polymer was relatively small in the present system.

Higher Molecular Weights and Higher Solid Contents

We targeted higher degrees of polymerization (DPs) in the polymerizations of MMA using 2-HEPhI (alkyl iodide) and BNI and NaI (catalysts). We obtained low-dispersity ($Đ$ =1.27-1.34) polymers at high monomer conversions (70-100%) in relatively short times (240-480 min) up to the M_n values of 18000-32000 (Table 2 (entries 3-5)).

We also targeted the higher solid content by increasing the amount of MMA monomer from 30 wt% to 40 and 50 wt% in the polymerization mixture (Table 2 (entries 6 and 7)). We obtained stable particles with up to high (95-100%) monomer conversions even in these high solid content systems. The polymerizations were also relatively fast (95-100% monomer conversions for 120-180 min). The result shows the high productivity of the present emulsion RCMP, which would be attractive for industrial application.

Functional Methacrylates

Besides MMA, we studied functional methacrylates, i.e., benzyl methacrylate (BzMA) with a benzyl group, glycidyl methacrylate (GMA) with an epoxide, and 2-hydroxyethyl methacrylate (HEMA) with a hydroxyl group, using 2-HEPhI as an initiating dormant species (Table 4 (entries 1-3)). The polymerization of BzMA completed in 1 h (monomer conversion = 100%), generating a polymer with M_n = 18000 and $Đ$ = 1.42. BzMA is more hydrophobic than MMA and the generated particles in the BzMA system would be easier to be stabilized. The hydrolysis of the epoxide of GMA is significant at high temperatures. Hence, we carried out the emulsion polymerization of GMA at 60 °C. The polymerization proceeded to a 64% monomer conversion for 2 h, attaining a relatively low $Đ$ (= 1.43) value with a nearly quantitative epoxide retention (Fig. S3 in ESI). The polymerization of HEMA (Table 4 (entry 3)) is an example of dispersion polymerization (not emulsion polymerization). HEMA (monomer) is soluble in water, but PHEMA (polymer) is not soluble in water. Therefore, mechanistically, the polymerization of HEMA can start in the water phase, and after reaching a critical chain length, the polymers would enter the particles. The polymerization would also proceed inside the particles. After 3 h, the monomer conversion reached 57%, a polymer with $Đ$ = 1.47 was generated.

Acrylates were not suitable to aqueous emulsion RCMP for obtaining low-dispersity polymers. While RCMPs of methacrylates require mild temperatures (e.g., 60 °C), RCMPs of acrylates require elevated temperatures (e.g., 110 °C), because the carbon-iodide bond of polyacrylate-iodide (secondary alkyl chain end) is stronger than that of polymethacrylate-iodide (tertiary alkyl chain end).[46,56] The required high temperature (above the boiling point of water (100 °C)) posed a difficulty in aqueous emulsion RCMPs of acrylates.

Table 4. Emulsion Polymerizations of Functional Methacrylates.[a]

Entry	Target DP[b]	Monomer	R-I	$[Monomer]_0/[2\text{-}HEPhI]_0/[NaI]_0/[BNI]_0/[V50]_0$ (mM)	T (°C)	t (h)	Conv (%)	M_n[c] ($M_{n,theo}$)[d]	$Đ$[c]
1	100	BzMA	2-HEPhI	8000/80/80/80/40	60	1	100	18000 (18000)	1.42
2	100	GMA	2-HEPhI	8000/80/80/80/40	60	2	64	14000 (8900)	1.43
3	100	HEMA	2-HEPhI	8000/80/80/80/40	60	3	57	10000 (7400)	1.47

[a]$[Monomer]_0/[emulsifier]_0/[water]_0$ = 30.0/3.3/66.7 (w/w/w). The emulsifier was a mixture of Tween80 and FES77 (3/1 (w/w)). [b]Target degree of polymerization (DP) at 100% monomer conversion as calculated according to $[Monomer]_0/[R\text{–}I]_0$. [c]PMMA-calibrated GPC values (DMF eluent). [d]Theoretical M_n value calculated according to ($[Monomer]_0/[R\text{–}I]_0$) × (monomer conversion) × (molecular weight of monomer).

Table 5. Emulsion Polymerization of St.

Entry	target DP[a]	R-I	Emulsifier[b]/water (wt%)	$[St]_0/[R\text{-}I]_0/[NaI]_0/[BNI]_0/[V50]_0$ (mM)	T (°C)	t (h)	conv (%)	M_n ($M_{n,theo}$)[c]	$Đ$
1	100	2-HEI	5.0/65.0	8000/80/160/160/80	60	4	82	18000 (8500)	1.24
2	100	2-HEI	5.0/65.0	8000/80/160/160/80	70	4	90	13000 (9400)	1.29
3	100	2-HEI	10.0/60.0	8000/80/160/160/40	70	3	92	16000 (9600)	1.25
4	100	2-HEI	10.0/60.0	8000/80/160/160/40	80	4	99	20000 (10000)	1.27
5	100	2-HEPhI	10.0/60.0	8000/80/160/160/40	70	4	92	18000 (9600)	1.24
6	100	2-HEPhI	10.0/60.0	8000/80/0/0/40	70	4	70	36000 (7300)	1.75

[a]Target degree of polymerization at 100% monomer conversion (calculated by $[St]_0/[R\text{-}I]_0$). [b]The emulsifier was Tween80. [c]Theoretical M_n value calculated according to ($[St]_0/[R\text{-}I]_0$) × (monomer conversion) × (molecular weight of St).

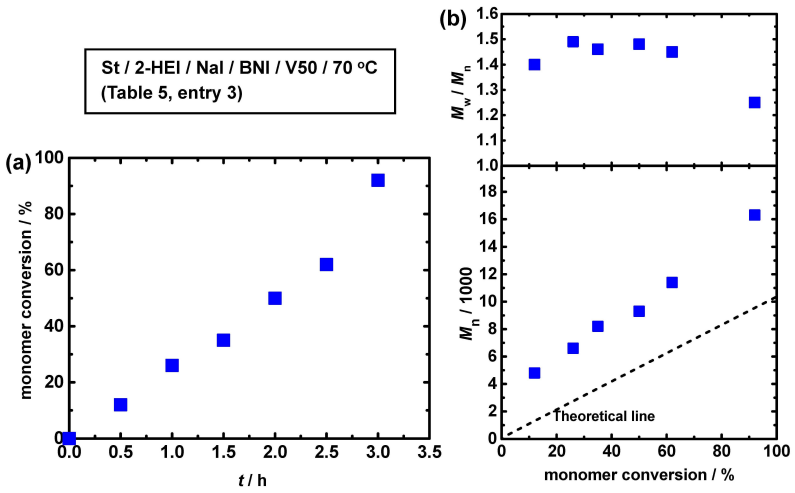

Fig. 7. Plots of (a) monomer conversion vs *t* and (b) M_n and M_w/M_n vs monomer conversion for the St/2-HEI/NaI/BNI/V50 system using Tween80 as an emulsifier (70 °C) (Table 5, entry 3): $[St]_0$ = 8 M; $[2\text{-HEI}]_0$ = 80 mM; $[NaI]_0$ = 160 mM; [BNI] = 160 mM; $[V50]_0$ = 40 mM.

Styrene

We studied another family of monomer, i.e., styrene (St). In contrast to the MMA system, where a combined use of Tween80 and FES77 was required, the styrene system required only the single use of Tween80. The ionic surfactant (FES77) was not required, because of the higher stability of the particles generated from the more hydrophobic St. No precipitation was observed by solely using Tween80.

We used 2-HEI as an alkyl iodide initiating dormant species and co-used NaI and BNI as catalysts. We heated a mixture of St (100 eq, 30.0 wt%), 2-HEI (1 eq), NaI (2 eq), BNI (2 eq), V50 (1 eq), Tween80 (5.0 wt%), and water (65.0 wt%) at 60 and 70 °C (Table 5 (entries 1 and 2)). The monomer conversion reached 82-90% in 4 h, generating a low-dispersity polymer (*Đ* = 1.24-1.29) in both cases. At the higher temperature of 70 °C, the polymerization was faster, and thus we further studied the amount of surfactant (Tween80) at 70 °C. We increased the amount of Tween80 from 5.0% (Table 5 (entry 2)) to 10.0% (Table 5 (entry 3) and Fig. 7). A high monomer conversion (92%) was attained in 3 h with 10% of Tween80, yielding a polystyrene with M_n = 16000 and *Đ* = 1.25. We further increased the temperature to 80 °C. The polymerization was fast and the monomer conversion reached 99% for 4 h. However, the M_n values nearly twice deviated from the theoretical values even at 80 °C, suggesting an approximately 50% initiation efficiency of 2-HEI. Thus, instead of 2-HEI, 2-HEPhI, which showed higher an initiation efficiency in the MMA system, was used in the St system at 70 °C (Table 5 (entry 5)). While the low *Đ* value (= 1.24) was attained, the M_n value still nearly twice deviated from the theoretical value. The reason for the deviation is not clear at this moment. Without the catalyst (NaI/BNI), the *Đ* value was large (1.75) (Table 5 (entry 6)), which is the iodide transfer (pure degenerative chain transfer) system. The degenerative chain transfer constant in the St system at 70 °C is 3.8,[67] which is relatively small and explains the observed large *Đ* value. The results (Table 5 (entries 5 and 6)) clearly show the effectiveness of the catalysts (NaI/BNI) to achieve the low dispersity. Thus, the emulsion RCMP of St generated low-dispersity polymers, although the initiation efficiency was approximately 50% for an unclear reason.

Conclusions

The emulsion RCMPs of MMA successfully generated stable polymer particles using the mixture of (non-ionic) Tween80 and (ionic) FES77 emulsifiers. The co-use of NaI and BNI as catalysts and the use of 2-HEPhI as an alkyl iodide initiator achieved nearly quantitative initiation and generated low-dispersity polymers (*Đ* = 1.1-1.3) at high (30-50%) contents of MMA monomer. The emulsion RCMPs of functional methacrylates and St also generated stable particles and low-dispersity polymers. The emulsion RCMP combines the advantages of emulsion polymerization such as efficient heat transfer, low viscosity, and high polymerization rate with those of RCMP such as no use of special capping agents or toxic catalysts. The high solid content, high chain-end fidelity, good monomer versatility achievable in the emulsion RCMP would also be attractive for polymer material design and industrial applications.

Conflicts of interest

There are no conflicts to declare.

Acknowledgements

This work was partly supported by National Research Foundation (NRF) Investigatorship in Singapore (NRF-NRFI05-2019-0001).

References

1 P. B. Zetterlund, S C. Thickett, S. Perrier, E. Bourgeat-Lami and M. Lansalot, *Chem. Rev.*, 2015, **115**, 9745−9800.
2 N. Corrigan, K. Jung, G. Moad, C. J. Hawker, K. Matyjaszewski and C. Boyer, *Prog. Polym. Sci.*, 2020, **111**, 101311.
3 M. F. Cunningham, *Prog. Polym. Sci.*, 2008, **33**, 365−398.
4 J. Qiu, S G. Gaynor and K. Matyjaszewski, *Macromolecules*, 1999, **32**, 2872−2875.
5 T. G. Ribelli, F. Lorandi, M. Fantin and K. Matyjaszewski, *Macromol. Rapid. Commun.*, 2019, **40**, 1800616.
6 R. Cordero, A. Jawaid, M-S. Hsiao, Z. Lequeux, R. A. Vaia and C. K. Ober, *ACS Macro Lett,* 2018, **7**, 459−463.
7 F. Lorandi, Y. Wang, M. Fantin and K. Matyjaszewski, *Angew. Chem. Int. Ed.*, 2018, **57**, 8270−8274.
8 R. W. Simms and M. F. Cunningham, *Macromolecules*, 2007, **40**, 860−866.
9 P. Gurnani and S. Perrier, *Prog. Polym. Sci.*, 2020, **102**, 101209.
10 I. Zaborniak and P. Chmielarz, *Macromol. Chem. Phys.*, 2019, **220**, 1900285.
11 Y. Kagawa, M. Kawasaki, P. B. Zetterlund, H. Minami and M. Okubo, *Macromol. Rapid Commun.,* 2007, **28**, 2354−2360.
12 T. Cuneo, X. Wang, Y. Shi and H. Gao, *Macromol. Chem. Phys.,* 2020, **221**, 2000008.
13 Y. Wang, S. Dadashi-Silab, F. Lorandi and K. Matyjaszewski, *Polymer,* 2019, **165**, 163−167.
14 X. Pan, M. Fantin, F. Yuan and K. Matyjaszewski, *Chem. Soc. Rev.*, 2018, **47**, 5457−5490.
15 Y. N. Zhou, J. J. Li, Y. Y. Wu and Z. H. Luo, *Chem. Rev.*, 2020, **120**, 2950−3048.
16 A. M. Doerr, J. M. Burroughs, S. R. Gitter, X. Yang, A. J. Boydston and B. K. Long, *ACS Catal.*, 2020, **10**, 14457−14515.
17 F. D'Agosto, J. Rieger and M. Lansalot, *Angew. Chem. Int. Ed.*, 2020, **59**, 8368−8392.
18 C. J. Ferguson, R. J. Hughes, B. T. T. Pham, B. S. Hawkett, R. G. Gilbert, A. K. Serelis and C. H. Such, *Macromolecules*, 2002, **35**, 9243−9245.
19 J. S. K. Leswin, J. Meuldijk, R. G. Gilbert and A. M. van Herk, *Macromol. Symp.*, 2009, **275–276**, 24−34.
20 Y. Li and S. P. Armes, *Angew. Chem. Int. Ed.*, 2010, **49**, 4042−4046.
21 Z. Jia, V. A. Bobrin, N. P Truong, M. Gillard, M. J. Monteiro, *J. Am. Chem. Soc.*, 2014, **136**, 5824−5827.
22 M. J. Derry, L. A. Fielding and S. P. Armes, *Prog. Polym. Sci.*, 2016, **52**, 1−18.
23 J. Zhou, H. Yao and J. Ma, *Polym. Chem.,* 2018, **9**, 2532−2561.
24 F. Jasinski, P. B. Zetterlund, A. M. Braun and A. Chemtob, *Prog. Polym. Sci.*, 2018, **84**, 47−88.
25 J. C. Foster, S. Varlas, B. Couturaud, Z. Coe and R. K. O'Reilly, *J. Am. Chem. Soc.*, 2019, **141**, 2742−2753.
26 N. Corrigan, J. Yeow, P. Judzewitsch, J. Xu and C. Boyer, *Angew. Chem. Int. Ed.*, 2019, **58**, 5170−5189.
27 C. Liu, C.-Y. Hong and C.-Y. Pan, *Polym. Chem.*, 2020, **11**, 3673−3689.
28 S. Li, G. Han and W. Zhang, *Polym. Chem.*, 2020, **11**, 4681−4692.
29 S. Pearce and J. Perez-Mercader, *Polym. Chem.*, 2021, **12**, 29−49.
30 H. Phan, V. Taresco, J. Penelle and B. Couturaud, *Biomater. Sci.*, 2021, **9**, 38−50.
31 S. C. Thickett and G. H. Teo, *Polym. Chem.*, 2019, **10**, 2906−2924.
32 N. J. W. Penfold, J. Yeow, C. Boyer and S. P. Armes, *ACS Macro Lett.*, 2019, **8**, 1029−1054.
33 S. Y. Khor, J. F. Quinn, M. R. Whittaker, N. P. Truong and T. P. Davis, *Macromol. Rapid. Commun.*, 2019, **40**, 1800438.
34 S. A. F. Bon, M. Bosveld, B. Klumperman and A. L. German, *Macromolecules*, 1997, **30**, 324−326.
35 J. Nicolas, B. Charleux, O. Guerret and S. Magnet, *Angew. Chem. Int. Ed.,* 2004, **43**, 6186−6189.
36 H. R. Lamontagne and B. H. Lessard, *ACS Appl. Polym. Mat.*, 2020, **2**, 5327−5344.
37 S. Tajbakhsh, F. Hajiali and M. Marić, *Ind. Eng. Chem. Res.,* 2020, **59**, 8921−8936.
38 M. Okubo, Y. Sugihara, Y. Kitayama, Y. Kagawa and H. Minami, *Macromolecules,* 2009, **42**, 1979−1984.
39 W. Fan, M. Tosaka, S. Yamago and M. F. Cunningham, *Angew. Chem. Int. Ed.,* 2018, **57**, 962−966.
40 X. Su, Y. Jiang, P. G. Jessop, M. F. Cunningham and Y. Feng, *Macromolecules,* 2020, **53**, 6018−6023.
41 J. Tonnar and P. Lacroix-Desmazes, *Polymer,* 2016, **106**, 267−274.
42 S. Sue-eng, T. Boonchuwong, P. Chaiyasat, M. Okubo and A. Chaiyasat, *Polymer*, 2017, **110**, 124−130.
43 J. Tonnar, P. Lacroix-Desmazes and B. Boutevin, *Macromolecules*, 2007, **40**, 186−190.
44 J. Tonnar, P. Lacroix-Desmazes and B. Boutevin, *Macromolecules*, 2007, **40**, 6076−6081.
45 A. Goto, A. Ohtsuki, H. Ohfuji, M. Tanishima and H. Kaji, *J. Am. Chem. Soc.,* 2013, **135**, 11131−11139.
46 X. Liu, C. G. Wang and A. Goto, *Angew. Chem. Int. Ed.*, 2019, **58**, 5598−5603.
47 C.-G. Wang, A. M. L. Chong, H. M. Pan, J. Sarkar, X. T. Tay and A. Goto, *Polym. Chem.*, 2020, **11**, 5559−5571.
48 J. Sarkar, L. Xiao and A. Goto, *Macromolecules,* 2016, **49**, 5033−5042
49 C.-G. Wang, F. Hanindita and A. Goto, *ACS Macro Lett.,* 2018, **7**, 263−268.
50 W. Mao, C.-G. Wang and A. Goto, *Polym. Chem.*, 2020, **11**, 53−60.
51 J. Sarkar, L. Xiao, A. W. Jackson, A. M. van Herk and A. Goto, *Polym. Chem.,* 2018, **9**, 4900−4907.
52 J. Sarkar, L. Xiao, A. W. Jackson, A. M. van Herk and A. Goto, *Polym. Chem.,* 2020, **11**, 3904−3912.
53 J. Sarkar, K. B. J. Chan and A. Goto, *Polym. Chem.*, 2021, **12**, 1060−1067.
54 A. Goto, T. Suzuki, H. Ohfuji, M. Tanishima, T. Fukuda, Y. Tsujii and H. Kaji, *Macromolecules,* 2011, **44**, 8709−8715.
55 C. Boyer, P. Lacroix-Desmazes, J. –J. Robin and B. Boutevin, *Macromolecules*, 2006, **39**, 4044−4053.
56 L. Lei, M. Tanishima, A. Goto, H. Kaji, Y. Yamaguchi, H. Komatsu, T. Jitsukawa and M. Miyamoto, *Macromolecules,* 2014, **47**, 6610−6618.
57 P. B. Zetterlund and M. Okubo, *Macromolecules*, 2006, **39**, 8959−8967.
58 R. W. Simms and F. Cunningham, *Macromolecules,* 2008, **41**, 5148−5155.
59 M. E. Thomson and F. Cunningham, *Macromolecules,* 2010, **43**, 2772−2779.
60 S. Tomoeda, Y. Kitayama, J. Wakamatsu, H. Minami, P. B. Zetterlund and M. Okubo, *Macromolecules*, 2011, **44**, 5599−5604
61 P. B. Zetterlund, *Polym. Chem.,* 2011, **2**, 534−549.
62 H. Fischer, *Chem. Rev.*, 2001, **101**, 3581−3610.
63 A. Goto and T. Fukuda, *Prog. Polym. Sci.*, 2004, **29**, 329−385.
64 A. Van der Lee, L. Hamon, Y. Holl and Y. Grohens, *Langmuir,* 2001, **17**, 7664−7669.
65 The density of Tween80 is 1.06 g/cm^3, https://www.sigmaaldrich.com/SG/en/product/sial/p1754, (accessed 9 June 2021).
66 The density of FES77 is 1.05 g/cm^3, https://chemical.carytrad.com.tw/uploads/1/2/3/8/123848866/tds_disponil_bes_fes_types_en.pdf, (accessed 9 June 2021).

67 A. Goto, K. Ohno and T. Fukuda, *Macromolecules,* 1998, **31**, 2809−2814.

Graphical Abstract

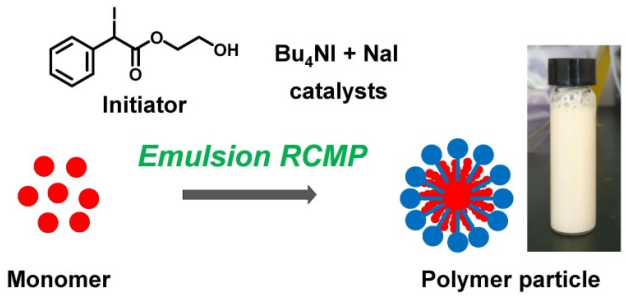

Textual Abstract: Aqueous emulsion polymerization via reversible complexation mediated living radical polymerization yielded low-dispersity poly(methyl methacrylate)s and polystyrenes.